# Ferromagnetic state in ultrathin orthorhombic CrAs films: Thickness, lattice distortion, and half-metallic contributions

Alexandre A. Araújo and Bernardo Laks
*Instituto de Física Gleb Wataghin, Universidade Estadual de Campinas, Caixa Postal 6165, 13083-970 Campinas, São Paulo, Brazil*

P. C. de Camargo
*Departamento de Física, Universidade Federal do Paraná, Caixa Postal 19091, 81531-990 Curitiba, PR, Brazil*
(Received 5 October 2006; published 20 November 2006)

Orthorhombic CrAs thin films were investigated using first-principles spin-polarized calculations in the full-potential linearized augmented plane-wave method. Our results consider two different geometry optimization processes and show that the ferromagnetic state is favored by *b*-axis expansion, being more stable than the antiferromagnetic state for film thickness below approximately 24 Å. The calculated maximum magnetic moment per formula unit is near $3\mu_B$ and decreases with increasing film thickness, in good agreement with the observed saturation magnetization. The electronic structure of very thin films with expanded *b* axis suggests a half-metallic behavior.

DOI: 10.1103/PhysRevB.74.172411 PACS number(s): 75.70.−i, 71.15.Ap, 71.15.Mb, 71.20.−b

The search for zinc-blende (ZB) half-metallic (HM) compounds among 3*d* transition metal chalcogenides is justified because of the high technological interest in the so-called spintronics, which requires polarized spin-injection devices.[1–3] A strong effort from the theoretical point of view, coupled to experimental evidence, has supported the view that ZB compounds of transition elements with atoms of groups V and VI may achieve epitaxial growth on semiconductors, preserving the HM characteristics for a few monolayers thickness.[4–6] In spite of the theoretical prediction that ZB CrAs on GaAs is ferromagnetic with half-metallic character, Etgens *et al.* found that CrAs grown on GaAs is ferromagnetic,[7] however, being orthorhombic near the interface. This orthorhombic ferromagnetic structure is mainly due to a *b*-axis deformation from 3.445 to 3.63 Å. Therefore, the main question to be answered concerns the origin of the magnetic behavior of orthorhombic CrAs films. This paper calculates the effects of lattice distortion and film thickness on the existence of ferromagnetism and half-metallic features.

Ferromagnetic phase stabilization depends on the characteristics of film. thickness and constraints due to the substrate lattice, in addition to interfacial features. In fact, ferromagnetism occurs for Cr, CrAs, or even arsenized Cr films prepared on GaAs substrates.[8] It is worth noticing that the magnetic moment per formula unit decreases as film thickness increases; it is quite generally accepted that the magnetic signal originates in the layer near the interface with GaAs.[7,9]

The orthorhombic ferromagnetic phase stability of a MnP-type (*Pnma* symmetry group) CrAs thin film is investigated, together with the magnetic moment and half-metallicity evolution as a function of film thickness and lattice parameters. We carried out energy minimization, within the scope of the Powell method,[10] as a function of all seven parameters (lattice and internal), searching for a new orthorhombic CrAs phase, based on the known bulk orthorhombic parameters.[11] This was performed from first-principles spin-polarized electronic band-structure calculations, based on the density functional theory,[12] using the general gradient approximation according to the Perdew-Burke-Ernzerhof parametrization.[13] For the self-consistent solution of the Kohn-Sham equations we have applied a full-potential linearized augmented plane-wave (LAPW) formalism, based on the WIEN code.[14,15] Relativistic effects are taken into account in the scalar approximation, but we have neglected spin-orbit coupling effects. The muffin-tin radii were chosen to be 2.3 Å for both Cr and As atoms. Inside the atomic spheres the charge density and the potential are expanded in spherical harmonics up to $l=6$. The maximum $l$ value for partial waves used inside atomic spheres is $l_{max}=10$. The nonspherical potential contribution to the Hamiltonian matrix has an upper limit of $l=4$. The plane-wave cutoff is $RK_{max}=7.0$ and we have used around 100 $k$ points in the first irreducible Brillouin zone. Self-consistency was considered attained when the difference in total energy per cell was smaller than $1\times10^{-7}$ Ry.

Thin films of different thicknesses were considered in the geometry optimization processes adopting the orthorhombic structure, where the **a** and **b** axes of the CrAs are in the plane parallel to the GaAs(001) surface and the **c** axes is perpendicular to the growth direction. This crystal orientation was chosen based on the experimental results found by Etgens *et al.*[7] Geometric and magnetic structures of orthorhombic CrAs, are shown in Fig. 1. In the *Pnma* symmetry group there are four Cr and four As inequivalent atoms. Thus, the ferromagnetic (FM), Fig. 1(a), and the three most likely magnetic orders involving Cr atoms, Figs. 1(b)–1(d), were considered in the total energy minimization procedures. Among the antiferromagnetic (AFM) configurations, the lowest total energy corresponds to the configuration shown in Fig. 1(c), and we called it the AFM state. We should mention that the paramagnetic phase corresponds to the highest-energy state.

The surface effects on the CrAs thin film were taken into account by introducing a film-vacuum interface in a supercell scheme, with a vacuum region corresponding to about six atomic layers of CrAs, considered large enough to prevent interaction between films. Substrate effects were assumed to constrain the *a* and *b* axes of CrAs to fixed values. Based on experimental evidence the possible interfacial reaction is considered to be negligible.[8]

Bulk and ultrathin films of 8, 12, 16, and 32 atomic lay-

 

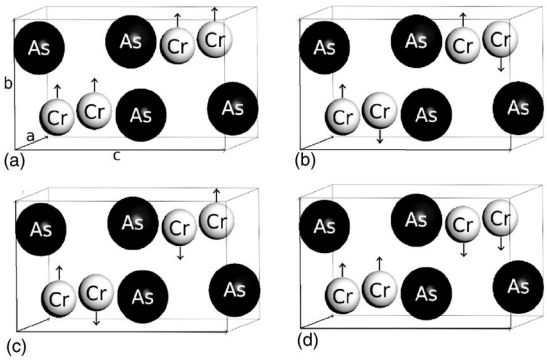


FIG. 1. Geometric and magnetic structures for orthorhombic CrAs in the *Pnma* symmetry group. The magnetic structures considered are a ferromagnetic state (a) and three antiferromagnetic states (b), (c), and (d).

ers, corresponding to thicknesses up to 24 Å, were investigated. All films have an equal number of Cr and As atoms and belong to a *Pnma* symmetry group, determined by three lattice parameters ($a$, $b$, and $c$) and four internal parameters ($x_{Cr}$, $x_{As}$, $z_{Cr}$, and $z_{As}$). The configuration that minimizes the total energy for orthorhombic thin films and bulk, as a function of all lattice and internal parameters, was calculated and compared, and from now on, this procedure is called free (F) minimization. The ferromagnetic total energy is also analyzed, considering the orthorhombic structure with $a$ and $b$ parameters parallel to the CrAs/GaAs interface with $a=5.74$ Å and $b=3.63$ Å,[7] and optimizing all the other parameters, calling this the restricted procedure (R). The most stable configuration for films and for bulk orthorhombic CrAs is found by comparing the total energy of all systems considered in this investigation.

The minimizations of total energy of CrAs, as a function of the structural parameters for bulk and thin films are shown in Fig. 2. In order to simplify the discussion, let us denoted by $\Delta E_R=(E_{AFM})_R-(E_{FM})_R$ the difference between the total antiferromagnetic energy and the total ferromagnetic energy

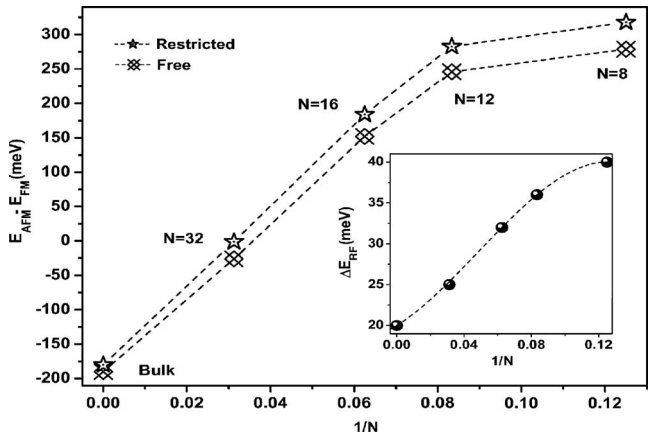


FIG. 2. Difference between antiferromagnetic ($E_{AFM}$) and ferromagnetic ($E_{FM}$) total energy (in meV) for orthorhombic CrAs thin films against $1/N$, where $N$ is the number of atomic layers. The points ($N=8$, 12, 16, 32, and bulk) were optimized for restricted ($\Delta E_R$) and free ($\Delta E_F$) geometries. The inset presents the difference between the restricted and free optimizations $\Delta E_{RF}=\Delta E_R-\Delta E_F$.

TABLE I. Optimized lattice and internal parameters of CrAs thin films with 8, 12, and 16 atomic layers in both free (F) and restricted (R) optimization processes.

| | $a$ | $b$ | $c$ | $x_{Cr}$ | $x_{As}$ | $z_{Cr}$ | $z_{As}$ |
|---|---|---|---|---|---|---|---|
| 8 layers F | 5.70 | 3.42 | 6.30 | 0.008 | 0.215 | 0.222 | 0.574 |
| 12 layers F | 5.70 | 3.54 | 6.20 | 0.006 | 0.214 | 0.218 | 0.586 |
| 16 layers F | 5.73 | 3.51 | 6.14 | 0.001 | 0.216 | 0.214 | 0.586 |
| 8 layers R | 5.74 | 3.63 | 6.13 | 0.009 | 0.210 | 0.218 | 0.589 |
| 12 layers R | 5.74 | 3.63 | 6.17 | 0.002 | 0.220 | 0.221 | 0.586 |
| 16 layers R | 5.74 | 3.63 | 6.15 | 0.005 | 0.220 | 0.220 | 0.586 |

minimized as a function of the structural parameters for the restricted optimization process, and, similarly, $\Delta E_F=(E_{AFM})_F-(E_{FM})_F$ for the free optimization process. Also let $\Delta E_{RF}=\Delta E_R-\Delta E_F$ be the difference between the differences of the restricted optimization and free optimization processes. In the case of bulk CrAs, the antiferromagnetic phase showed lower total energy than the ferromagnetic phase, that is, $\Delta E_R<0$ and $\Delta E_F<0$, as expected. It is important to notice that the total energy difference between the FM and AFM phases for restricted optimization is smaller than in the case of free optimization, that is, $\Delta E_{RF}>0$. Thus, a $b$-axis expansion contributes to stabilization of a ferromagnetic phase; however, this is less stable than the bulk antiferromagnetic phase.

The surprising result occurs for thin films, where the ferromagnetic phase is more stable considering the restricted or free optimization process, as shown in Fig. 2. The most relevant feature is the intrinsic thickness effect that, for all considered thicknesses the difference between the total energies of FM and AFM phases increase when we keep $a$ and $b$ fixed ($\Delta E_{RF}$ is always positive). In conclusion, the ferromagnetic phase is stabilized as the thickness decreases, which agrees with most literature results.[7,8] Moreover, as the $\Delta E_R$ ($\Delta E_F$) values become smaller as the film thickness increases a phase transition from ferromagnetic to antiferromagnetic is expected at some finite thickness, when the bulk antiferromagnetic CrAs is recovered. Our theoretical results indicate that the magnetic phase transition occurs for 32-atomic-layer films, corresponding to a thickness bellow 24 Å, in very good agreement with experimental results.[7] The inset in Fig. 2 presents the difference between restricted and free optimization $\Delta E_{RF}=\Delta E_R-\Delta E_F$. The results suggest an increase of $\Delta E_{RF}$ as the thickness decreases, showing a saturation below $N=8$.

Now, the most interesting question is to find out what are the most sensitive parameters that cause the magnetic phase transition. Table I compares optimized values for thin films with 8, 12, and 16 atomic layers, showing that the $b$ axis is the one that changes most significantly. This larger modification of the $b$ axis also agrees with experimental results,[7] following the assumption of Etgens *et al.* that the role of the GaAs substrate is, mainly, to enlarge the $b$ axis as compared to that of bulk CrAs. The $c$ parameter in Table I is to be understood as the lattice parameter along the $c$ axis, when the vacuum region is not considered, therefore giving an idea of how it changes relative to the bulk.

Another relevant feature is concerned with the effect of

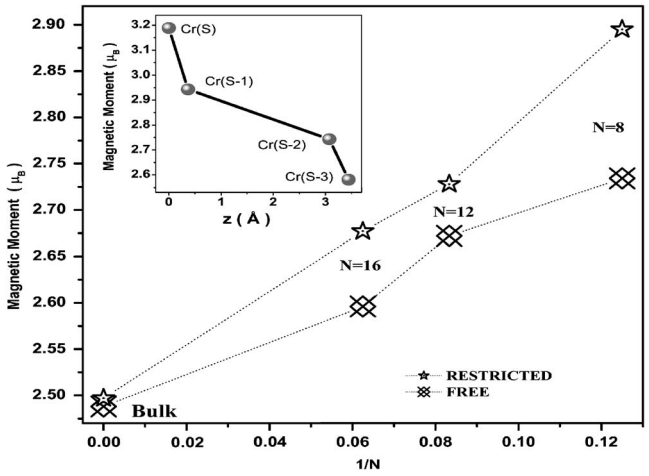


FIG. 3. Magnetic moment per formula unit for CrAs films as a function of the inverse of the number of atomic layers ($N$). The inset presents the magnetic moment at Cr atoms for restricted optimization, starting from the most external toward the inner layers, up to the fourth Cr, considering a film with $N=16$.

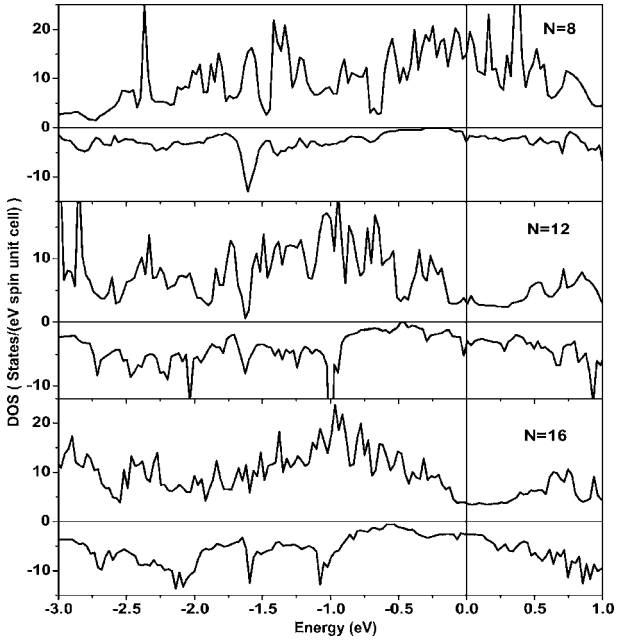


FIG. 4. Spin-resolved densities of states for CrAs films, with $N=8$, 12, and 16 layers in the restricted optimization. An energy gap is observed near the Fermi level for $N=8$.

the substrate strain and film thickness on the spin polarization. Figure 3 shows the values of magnetic moment for a unit cell of CrAs as a function of the inverse of film thickness, considering films with $N$ atomic layers for restricted and free optimization processes. Both processes show a clear increase of magnetization as the thickness of the film decreases. For the restricted optimization, the magnetization changes from $2.5\mu_B$ (bulk) to $2.9\mu_B$ (eight-atomic-layer film). The substrate effect increases the magnetic moment of Cr atoms up to 6.5%.

The magnetic moments for Cr atoms from surface to inner layers, in the restricted optimization for the film with $N=16$, can be seen in the inset of Fig. 3. Our results show that the most external Cr atom has the highest magnetic moment, reaching values above $3\mu_B$, while the next Cr atom has about $2.9\mu_B$. The values of the magnetic moment at the most external Cr atoms for 8 and 12 atomic layers are also close to $3\mu_B$. The corresponding values for the free optimization (not shown) are a little smaller, but the behavior is very similar.

From the applications point of view the half-metallic nature of this CrAs films is the most relevant aspect, so that the electronic density of states is now considered. The curves of spin-polarized density of states (DOS) for the three films (8, 12, and 16 layers) are presented in Fig. 4, considering the restricted optimization, showing that spin-up electrons have a metallic behavior for all cases. However, in the case of spin-down electrons there is a decreasing density of states near the Fermi level, so that, for eight atomic layers film ($N=8$), in the restricted optimization, a small energy gap appears just below the Fermi level. The same decreasing tendency of the density of states near the Fermi level (not shown) is also observed for free optimization; however, no energy gap is reached even for the eight-atomic-layer film. These results indicate that a half-metallic behavior is likely to occur for very thin films with expanded $b$ axis. Therefore, the orthorhombic ferromagnetic phase of ultrathin CrAs films brings a quite strong change on the electronic structure. The exchange splitting of the $d$ bands produces the ferromagnetism and further pushes to higher energy the minority-spin bands above the Fermi level. This is the origin of the energy gap (in the eight-atomic-layer film) and of the valley (in the other films) near the Fermi level on the minority-spin density of states, as shown in Fig. 4.

To make clear the discussion about the electronic structure of the orthorhombic ferromagnetic CrAs phase, and to get some insight into the bonding properties, we present in Fig. 5 spin-dependent energy-resolved contour plots of the charge density along a plane perpendicular to the $b$ axis for the film with 16 atomic layers. This plane crosses both Cr and As atoms. We selected three energy regions in the occupied band. In the first region, between −6.0 and −4.0 eV, the hybridization of the $4p$ As and the $3d$ Cr orbitals results in an almost equal participation of the electrons from both atoms. The contour plot for the majority spin, shown in Fig. 5(a), clearly suggests the bonding character of the electrons on this energy range. The result of the minority spin (not shown) is practically the same as obtained for the majority spin. Moving the spectrum toward higher-energy regions, we have found an increase in the charge concentration around Cr atoms sites, and a smaller number of spin-down electrons relative to the number of spin-up electrons, consistently with the fact that the minority-electron $d$ states are shifted significantly with respect to majority-electron $d$ states by the exchange interaction. Our results for the energy region between −3.0 and −1.0 eV are shown in Figs. 5(b) (spin up) and 5(c) (spin down). We have noticed that, in this energy region, the majority electrons occupy nonbonding states, while the minority electrons occupy bonding states. In the third energy region, near the Fermi energy, the number of minority electrons drops drastically, as compared to the majority electrons, but both spin-polarized states present a nonbonding character

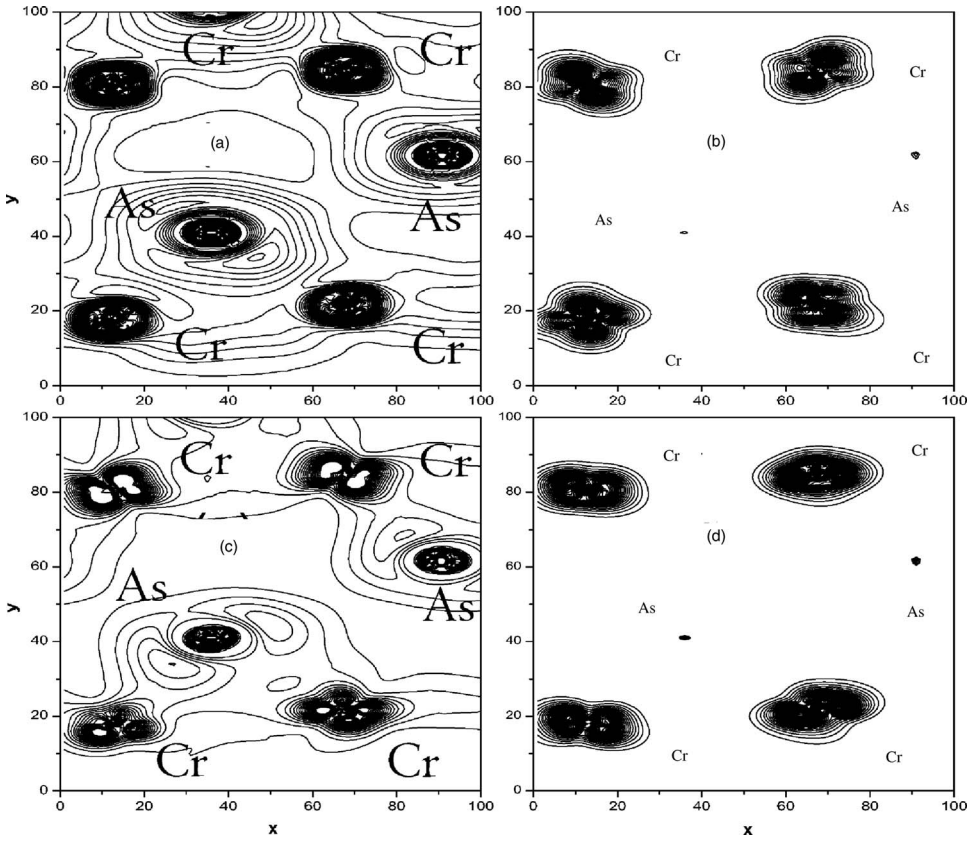


FIG. 5. Contour plots of charge densities for selected states of ferromagnetic CrAs film with $N=16$ layers. (a) Occupied majority-spin states, in the energy range $-6.0$ to $-4.0$ eV, showing evidence of As-Cr bonding character. (b) and (c) Occupied majority and minority-spin states, respectively, between $-3.0$ and $-1.0$ eV. While majority-spin states present a nonbonding character, the minority-spin states present a bonding character. (d) Occupied majority-spin states near the Fermi level, showing nonbonding character.

and the contour plot of the majority electrons can be seen in Fig. 5(d).

In summary, we have performed an optimization process by minimization of the total energy as a function of the structural parameters for bulk and ultrathin films of orthorhombic CrAs. The results show that a ferromagnetic phase is stabilized for very thin films. The theoretical results predict a ferromagnetic to antiferromagnetic phase transition, when the *b* axis expands to reach the Etgens *et al.* value for a film thickness around 32 atomic layers. In addition, the film thickness plays two fundamental roles. The first is to stabilize the ferromagnetic phase with increasing magnetic moment as the thickness decreases. The second is to modify the total density of states at the Fermi level, which shows a gap for spin down, but metallic behavior for spin up, as a typical half-metallic material. The calculation shows also that the magnetic moment at Cr atoms increases as surface is approached, reaching values slightly above $3\mu_B$, at the surface of very thin films, decreasing quickly as thickness increases. The optimized lattice parameters are in good agreement with those of Etgens *et al.*, and clearly indicate that *b*-axis expansion is the main lattice parameter that causes the magnetic ordering. The magnetic moment per formula tends to $3\mu_B$ and quickly decays as the thickness of the film increases. Finally, our results indicate the future possibility of stabilization of a half-metallic regime in orthorhombic room temperature ferromagnetic ultrathin CrAs films.

The authors thank the Brazilian agencies FAPESP, Capes, and CNPq for financial support and CENAPAD SP for computational support.

[1] G. Prinz, Science **282**, 1660 (1998).
[2] S. A. Wolf, D. D. Awschalom, R. A. Buhrman, J. M. Daughton, S. von Molnar, M. L. Roukes, A. Y. Chtchelkanova, and D. M. Treger, Science **294**, 1488 (2001).
[3] R. A. de Groot, F. M. Mueller, P. G. van Engen, and K. H. J. Buschow, Phys. Rev. Lett. **50**, 2024 (1983).
[4] M. Shirai, Physica E (Amsterdam) **10**, 143 (2001).
[5] H. Akinaga, T. Manago, and M. Shirai, Jpn. J. Appl. Phys., Part 2 **39**, L1118 (2000).
[6] J. H. Zhao, F. Matsukura, K. Takamura, E. Abe, D. Chiba, and H. Ohno, Appl. Phys. Lett. **79**, 2776 (2001).
[7] V. H. Etgens, P. C. de Camargo, M. Eddrief, R. Mattana, J. M. George, and Y. Garreau, Phys. Rev. Lett. **92**, 167205 (2004).
[8] D. H. Mosca, P. C. de Camargo, J. L. Guimarães, W. H. Scheiner, A. J. A. de Oliveira, P. E. N. Souza, M. Eddrief, and V. H. Etgens, J. Phys.: Condens. Matter **17**, 6805 (2005).
[9] H. Ofuchi, M. Mizuguchi, K. Ono, M. Oshima, H. Akinaga, and T. Manago, Nucl. Instrum. Methods Phys. Res. B **199**, 227 (2003).
[10] M. J. D. Powell, Comput. J. **7**, 155 (1964).
[11] H. Boller and A. Kallel, Solid State Commun. **9**, 1699 (1971).
[12] W. Kohn and L. J. Sham, Phys. Rev. **140**, A1133 (1965).
[13] J. P. Perdew, K. Burke, and M. Ernzerhof, Phys. Rev. Lett. **77**, 3865 (1996).
[14] P. Blaha, K. Schwarz, and J. Luitz, computer code WIEN 97 (Vienna University of Technology).
[15] P. Blaha, K. Schwarz, P. Sorantin, and S. B. Trickey, Comput. Phys. Commun. **59**, 399 (1990).